



## The Characterization of Heterogeneous Nanocatalyst of Biohydroxyapatite-Lithium and its Application for Converting *Malapari* Seed Oil (*Milletia pinnata* L.) to Biodiesel

I NENGAH SIMPEN\*, I MADE SUTHA NEGARA and NI MADE PUSPAWATI

Department of Chemistry, Faculty of Mathematics and Natural Sciences,  
Udayana University Kampus Bukit Jimbaran, Badung-Bali 80361, Indonesia.

\*Corresponding author E-mail: ngahsimpen@yahoo.com

<http://dx.doi.org/10.13005/ojc/3404015>

(Received: July 10, 2018; Accepted: August 01, 2018)

### ABSTRACT

Heterogeneous nanocatalyst of biohydroxyapatite-lithium (HA-Li) has been prepared through modification of HA extracted from bovine bone waste with Li at various calcination temperatures (400-700°C). Characterizations of the heterogeneous catalysts were including surface acidity-basicity, functional groups, BET surface area, particle size, and surface morphology. Optimization of catalyst ratios (1-7%) with the best characterization was applied for converting *Malapari* seed oil (*Milletia pinnata* L.) to biodiesel. The characterization results showed that HA-Li catalyst calcinated at 600°C had the highest surface basicity and Lewis acid sites revealing specific functional group of O-Li at wavenumber of 1612.49 cm<sup>-1</sup>. BET surface area of HA-Li catalyst decreased with increased average particle size. SEM analysis suggested that morphology of catalysts formed stack of agglomerates. The highest yield of biodiesel obtained on a catalyst ratio of 5% was 88.16%. GC-MS analysis showed 10 peaks, and 5 of the peaks exhibiting the highest percentage area were identified as methyl oleic, methyl palmitic, methyl erusic, methyl stearic, and methyl linoleic.

**Keywords:** Biohydroxyapatite-lithium, Nanocatalyst, *Malapari* seed oil, Biodiesel.

### INTRODUCTION

Research of conversion *Malapari* seed oil (*Milletia pinnata* L.) to biodiesel is predominantly using a liquid based homogeneous catalyst (NaOH or KOH). Biodiesel production using homogeneous catalysts has several disadvantages, namely the separation and purification of products are considered to be less environmentally benign and

economical<sup>1</sup> and tend to be corrosive when it used on machines<sup>2</sup>. The use of solid base catalysts (heterogeneous catalysts) is selected to overcome the deficiency of the homogeneous catalyst properties. Heterogeneous catalysts have advantages over homogeneous catalysts, such as the production of biodiesel using few units of operation with ease of separation and purification of products<sup>3</sup> as well as non-corrosive, non-toxic, and can be regenerated<sup>4</sup>.



Currently, the heterogeneous catalyst developed by many researchers is calcium oxide. However, CaO has a weakness that is rapidly hydrated and easily carbonated at room temperature and quickly forms the paste when mixed with methanol, therefore the role of the catalyst becomes unstable. As a result, conversion of soybean oil to biodiesel is low<sup>5</sup>. The ideal heterogeneous catalyst for the manufacture of biodiesel must, amongst other things, be stable against temperature changes, large alkaline sites, large pores, hydrophobic surfaces (dislikes of water), and cheap<sup>6</sup>. Therefore, heterogeneous catalysts developed and based on CaO are hydroxyapatite extracted from bovine bone handicraft waste. Given the sculpture for souvenirs, made from raw bovine bone is currently quite developed in Bali. In addition to the raw material of souvenir statues, bones are also widely used as raw material for making dice, buttons, bracelets, and knife stalks. Handicrafts made from raw bovine bone, produced waste in the form of bone powder of at least 2 kilograms per day at each place of bone handicraft. The resulting waste is simply thrown away, whereas from its chemical composition, bone greatly supports its potential enhancement<sup>7</sup>. Chemical compositions, more than 70% are hydroxyapatite biomineral  $[\text{Ca}_{10}(\text{PO}_4)_6(\text{OH})_2]$ <sup>8</sup>, have the potential to be used as heterogeneous catalysts because their constituent structures are porous, inert<sup>9</sup>, and serves as an active sites provider, especially the surface base as it contains the OH site<sup>10-11</sup>. However, it is necessary to improve the performance of hydroxyapatite by modification using lithium (Li)<sup>10</sup>. Modifying with Li in solid state reaction at various calcination temperature has several advantages, such as high activity, resistance to steam disturbance (acid, base, and neutral), and can be recycled to become more economical<sup>5</sup>. Utilization of synthetic heterogeneous  $\text{Li}_2\text{SiO}_3$  catalyst for converting soybean oil to biodiesel has been done<sup>5</sup>, that Li acts as an active site enhance and increased percentages can increase biodiesel yields. In addition, to open the base site on the surface, the rearrangement of the surface and its constituent atoms in addition to eliminate water and carbon dioxide required initial processing using variation in the calcination temperatures<sup>12-13</sup>.

The *Malapari* seed oil is one of the main raw materials of biodiesel production which is currently being studied and developed, especially in India

and Australia. The *Malapari* seed oil is not edible oil and so its availability is more secure than food oils, such as palm oil, coconut oil, soybean oil, pecan oil, and others. In Bali, many *Malapari* plants are found in Lovina Beach, Buleleng and Nusa Penida Beach, Klungkung. After extraction, *Malapari* seed from Lovina Beach, Buleleng produced the highest yield of 32% (dry weight, %w/w)<sup>14</sup>.

In order to produce the expected biodiesel yield, the characteristics of heterogeneous catalyst used must have a high surface basicity, functional groups required for the active sites, large surface area, and other characteristics necessary for its application for converting *Malapari* seed oil to the biodiesel.

## MATERIALS AND METHODS

### Materials

The bovine bones of handicraft waste were collected from Tampak Siring Gianyar Bali, the *Malapari* seeds were collected from Lovina Beach Buleleng Bali, the filtration with usual filter paper and Whatman filter paper 42. The chemicals of sodium hypochloride, sodium hydroxide, and hydrogen peroxide were reagent grade diluted by distilled water. Other chemicals were reagent grade ( $\text{Li}_2\text{CO}_3$  and methanol) and technical grades.

### METHODS

#### Extraction of biohydroxyapatite

Bovine bone waste was washed with water to clean any impurities and then dried in oven at 110-120°C for 12 hours. The dried bovine bone was crushed to get a powder, and sieved to obtain size of 0.50 to 0.25 mm. Subsequently, bovine bone was soaked in 10% NaOCl for 24 h then washed with distilled water and boiled in 5% NaOH for 3 hours. It was then washed with distilled water and resoaked in 10% of  $\text{H}_2\text{O}_2$  for 24 hours. The treated bovine bone was subsequently calcinated at 650°C for 3 hours. The hydroxyapatite powder obtained was sterilized at 100-150°C for 3 h<sup>7,9</sup>. Afterward, biohydroxyapatite was labelled as HA and stored in decicator and it was ready to be used for further experiments.

#### Modification of biohydroxyapatite with lithium

Modification of HA with lithium was done by varying the calcination temperatures at 400°C

(HA-Li400 labelled), 500°C (HA-Li500 labelled), 600°C (HA-Li600 labelled), and 700°C (HA-Li700 labelled) and HA without modification as control for comparison. The modification was done in solid state reaction. One (1.0) g of each HA was mixed with  $\text{Li}_2\text{CO}_3$  (0.23 g Li) on porcelain cup, then dehydrated at 200°C for 30 minutes<sup>15</sup>. Subsequently, calcination was carried out for 4 h at 400, 500, 600, and 700°C.

### Characterization of Catalysts

The HA-Li and HA catalysts were characterized for their physical and chemical properties. BET (Brunauer, Emmett and Teller) surface area and average particle size were measured by gasorption nitrogen analyzer (Micromeritics TriStar II 3020 version 2.00), basicity-acidity by acid-base titrations, functional groups by Fourier transform infrared spectroscopy (FTIR, Shimadzu/IR Prestige-21), and surface morphology by scanning electron microscopy (SEM, JEOL JSM-6510 LA/Japan). The optimum calcination temperature was determined from the best characteristics of catalyst obtained with the highest surface basicity and specific surface area and functional groups as the active sites. The best characteristics of HA-Li catalyst selected was then tested for its capability in converting Malapari seed oil (*Milletia pinnata* L.) to biodiesel and compared with HA catalyst.

### Conversion of Malapari seed oil (*Milletia pinnata* L.) to Biodiesel

The Malapari seed oil (extracted from Malapari seed by soxhlet extraction method)<sup>14</sup> initially was filtered to clean any impurities, then heated at 110°C for 30 min. to remove water content. After the heating process, the oil was allowed to cool at 50-55°C<sup>16</sup>. Next step was the transesterification reaction of oil using HA-Li best catalyst to produce

biodiesel. In order to obtain the highest yield of biodiesel, the ratio of HA-Li catalyst to the Malapari seed oil was varied (1, 3, 5, and 7% w/w HA-Li to the oil). Each percentage ratio of the HA-Li catalysts (1, 3, 5, and 7%) firstly was dissolved into methanol with 9:1 molar ratio of methanol to oil and stirred for 20 minutes<sup>17</sup>. The HA-Li methanol mixture was slowly added to the Malapari seed oil. The reaction was carried out at 65°C for 150 min. with constant stirring<sup>18</sup>. After the reaction completion, the heating was stopped and the reaction product was allowed to cool at room temperature and weighed. The product was transferred to a separating funnel and left for 12 h to form 3 layers. The top layer (layer 1) was an unreacted methanol residue, layer 2 (middle) was a biodiesel, and the bottom layer was a glycerol and the catalyst. The biodiesel layer was collected and filtered to obtain a clear oil. The oil was further distilled at temperature of 65°C to remove the remaining methanol. The resulting biodiesel was then weighed and the yield was calculated.

### Characterization of Biodiesel

The highest yield of biodiesel obtained was further analysed for its methyl ester content using gas chromatography-mass spectrometry (GC-MS-QP2010 Ultra Shimadzu) to confirm that transesterification of the oil to biodiesel have been occurred. The physical and chemical properties of Malapari seed oil as feedstock and biodiesel were determined and compared with European Standard (EN 14214).

## RESULTS AND DISCUSSION

### Surface acidity and basicity of catalysts

The results of surface basicity, amount of base sites, total acidity, Lewis acidity, and amount of Lewis acidity of the catalysts were summarised in Table. 1.

**Table 1: Surface basicity, amount of base sites, total of acidity, Lewis acidity, and amount of Lewis acid sites of catalysts**

Type of catalysts	Basicity (mmol/g)	Amount of base sites (x10 <sup>20</sup> sites/g)	Total acidity (mmol/g)	Lewis acidity (mmol/g)	Amount of Lewis acidity (x10 <sup>20</sup> sites/g)
HA	2.1803	13.1319	0.0522	0.00	0.00
HA-Li400	0.3287	1.9798	0.4815	0.4293	2.5857
HA-Li500	1.2304	7.4070	0.8085	0.7563	4.5552
HA-Li600	1.5363	9.2531	0.8387	0.7865	4.7371
HA-Li700	1.4019	8.4436	0.4512	0.3990	2.4032

As seen in Table. 1, the surface basicity and the number of base sites HA catalyst were higher than HA-Li catalysts, but it did not contain Lewis acid sites. The HA-Li600 catalyst revealed the highest surface basicity, number of base sites, Lewis acidity and also number of Lewis acid sites as compared to other HA-Li catalysts type. The surface basicity was influenced by the number of an O-H (anion) and Lewis acid sites by a Li (cation) groups presented in the catalysts. Rearrangements of this groups on the surface of its atoms constituent occurred during the calcination process with variation of temperatures affecting the number of sites and natural character of the bases<sup>13</sup>. The concentration of Bronsted bases sites as negative oxygen ions or anions (protons acceptor) and Lewis acidity sites as cations or electron acceptor<sup>6</sup> in the active site of heterogeneous metal oxide catalysts played an important role in the transesterification reactions for producing biodiesel. Bronsted base sites and Lewis acidity were also responsible for the formation of anion methoxide after the heterogeneous catalyst interacted with methanol. The anionic methoxide that has formed will react with the triglyceride molecules of the oil to produce its methyl ester derivative. The presence of Bronsted acid sites in the hydroxyapatite (HA) extracted from bovine bone waste can be seen from the FTIR spectra data. The characteristic of Bronsted acid sites appeared at wavenumbers of 1300-1550  $\text{cm}^{-1}$  after adsorbing ammonia vapor<sup>7</sup> but

it did not exhibit wavenumber corresponding to Lewis acid sites. Therefore, the Lewis acidity and the number of Lewis acid sites content in the lithium modified HA (HA-Li) were obtained from subtraction of HA-Li total acidity and the HA total acidity (Table. 1).

### Functional groups of catalysts

As shown in Fig.1, typical functional groups of O-Li in modified HA at temperatures of 400, 500, 600, and 700°C (HA-Li400, HA-Li500, HA-Li600, and HA-Li700 respectively) appeared at wavenumber of 1612.49  $\text{cm}^{-1}$ , indicating a vibration of O-Li and this also seen in the  $\text{Li}_2\text{CO}_3$  but did not in the HA catalyst. The spectrum of O-H group on the HA-Li catalysts became broader and the intensity decreased (15.768-21.929) compared to HA (32.066) and similar to intensity of O-H in  $\text{Li}_2\text{CO}_3$  (15.761). The broadener and low intensity of the O-H spectrum may due to the number of O-H groups as the characteristic of Bronsted base sites decreased. This was supported by research of Betancur *et al.*, (2013), that alkaline treated bone (deproteination) produced a broad-spectrum O-H stretching, whereas calcinated bone was indicated by a sharp stretching O-H spectrum and an increased number of O-H bending<sup>19</sup>.

### Surface area and particle size of catalysts

BET surface area and average particle size of the catalyst were summarized in Table. 2. The average particle size was calculated using the equation  $D = 6/(\rho S_{\text{BET}})$ , where D was the mean particle size (nm),  $\rho$  was the density of pure HA ( $3.16 \text{ g/cm}^3$ ), and  $S_{\text{BET}}$  was the specific surface area ( $\text{m}^2/\text{g}$ )<sup>20</sup>.

**Table 2: BET surface area and average particle size of catalysts**

Type of catalysts	BET surface area ( $\text{m}^2/\text{g}$ )	Average particle size (D, nm)
HA	19.3820	97.96
HA-Li400	10.5660	179.70
HA-Li500	7.2031	263.59
HA-Li600	10.5147	180.58
HA-Li700	4.8348	392.72

As summarised in Table. 2, the temperature of calcination affected the surface area and particle size of the Li modified catalyst. In general, BET surface area decreased (10.5660 to 4.8348) and average particle size increased (179 to 392 nm) when



**Fig. 1. FTIR spectra of  $\text{Li}_2\text{CO}_3$  and catalysts**

the temperature of calcination increased compared to the nano particle size (97 nm) of HA catalyst with exception for Ha-Li calcinated at 600°C. This results confirmed that Li has entered into the structure of HA. The HA-Li modified catalyst calcinated at 500°C exhibited a relatively smaller surface area than the calcinated at 400°C, with a larger particle size. This indicated that increasing the calcination temperature resulted in the rearrangement of the structure which occurred in solid state reaction. It was interesting to note that the surface area and particle size of the Li-modified catalyst calcinated at 600°C had similar value to HA-Li at 400°C (toward the average size of the nanoparticles) but further increased. The calcination temperature of 700°C reduced the BET surface area and increased the average particle size. Hence, the optimum calcination temperature of HA-Li modified catalyst was at 600°C. Variation in calcination temperatures can changed the arrangement of surface atoms, thus affecting the structure of the modified catalysts including surface area and particles size<sup>12</sup>.

### Surface morphology of catalysts

The SEM analysis (Fig. 2) provided an illustration of Li dispersion in a HA matrix. Generally, the homogeneity of Li dispersion on the

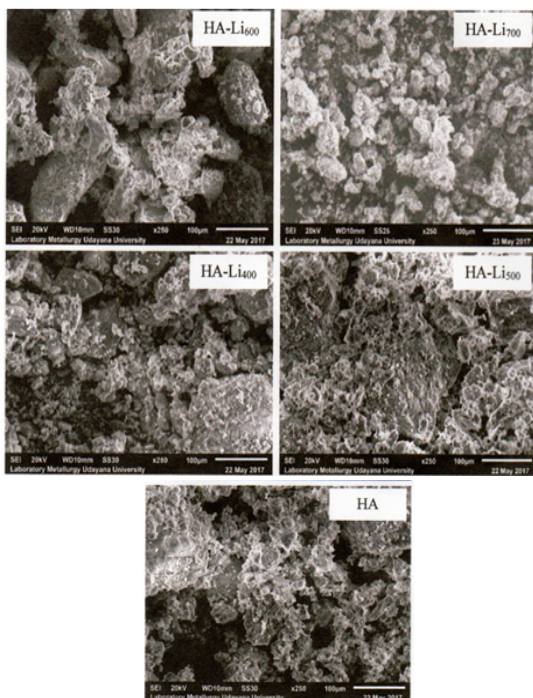


Fig. 2. Surface micrograf of catalysts at 250x enlargement

variation of calcination temperatures in HA can be observed. The SEM results suggested that surface morphology of HA and HA-Li catalysts formed stack of agglomerates<sup>21</sup>. The pores size of the HA-Li400 and HA-Li500 catalysts were shrunk and visibly covered. While, the HA-Li600 catalyst had more open pores and uniform than others, hence the particles become unity one in another. However, the particle in the HA-Li700 catalyst tend to separate from one another therefore the formation of pores became interconnected. This phenomenon is in good agreement with the result of catalysts BET surface area (Table. 2), showed that increasing particle size of catalysts with the calcination temperatures of 400, 500, and 700°C<sup>21</sup> but decreasing at calcination temperature of 600°C. HA-Li600 catalyst had pore rearranged after the calcination temperatures of 400 and 500°C, but at 700°C was damaged.

### Tests of catalytic activity for converting *Malapari* seed oil to biodiesel

Based on the results of the characterization of surface basicity and acidity, surface area, FTIR, and SEM, the best Li modified HA catalyst was the HA-Li600. The HA-Li600 catalyst was further tested for its catalytic ability for converting *Malapari* seed oil to biodiesel in transesterification reaction, with variation of catalyst ratios 1, 3, 5, and 7% to the oil.

Table. 3: Yield of biodiesel with variation of catalyst ratios to *Malapari* seed oil

Type of catalysts	Yield (%) with variation of catalyst ratios			
	1%	3%	5%	7%
HA	34.89	35.77	38.46	38.42
HA-Li600	70.06	74.35	88.16	87.66

As shown in Table. 3, the yield of biodiesel obtained increased as the ratio of catalysts used increased. The used of 1%, 3%, and 5% ratio of catalyst yielded 70.06, 74.35, and 88.16 % biodiesel respectively. However, increasing the ratio of catalyst to 7%, the yield of biodiesel slightly decreased to 87.66% suggesting that at this ratio the catalyst had no more capability to improve the conversion of oil to the biodiesel as it was expected. Therefore, the highest biodiesel yield of 88.16% was obtained using HA-Li600 with 5% of catalyst ratio to oil.

### Characterization of methyl esters content in the highest biodiesel yield

The chromatogram of GC-MS analysis as depicted in Fig.3. showed 10 peaks corresponding to fatty acid methyl ester (FAME). Based on the

GC-MS (Willey7.Lib) base data, 5 of the peaks with the highest percentages area were identified as methyl oleic (25.37%), methyl palmitic (22.00%), methyl erusic 13.15%), methyl stearic (11.16%), and methyl linoleic (7.53%).

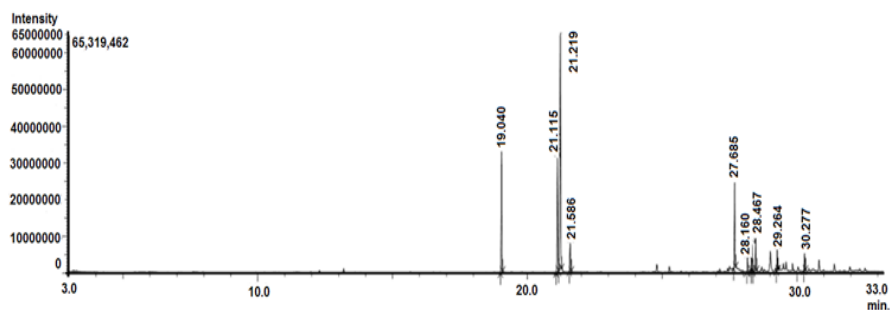


Fig. 4. Chromatogram of GC-MS analysis of biodiesel

### Characterization of physical and chemical properties of both *Malapari* seed oil and biodiesel

The data in Tabel. 4, physical and chemical properties of *Malapari* seed oil were higher than European Standard (EN 14214), the only iodine value was suited the EN 14214. Therefore, *Malapari* seed oil can not be applied directly for diesel fuels. Converting *Malapari* seed oil to biodiesel, its physical and chemical properties (Tabel. 5) can be concluded that several characteristics were agreement with those reported by EN 14214 standard for biodiesel<sup>21</sup>.

Table 4: Physical and chemical properties of *Malapari* seed oil as feedstock

Property	Unit	Value
Density	kg/m <sup>3</sup>	959
Kinematic viscosity (40°C)	mm <sup>2</sup> /s	27.033
Free fatty acid (FFA)	%	1.14
Iodine value	mg I <sub>2</sub> /100g	85.47
Water content	%	12.40

Table 5: Physical and chemical properties of biodiesel

Property	Unit	Value	EN 14214 standard
Density	kg/m <sup>3</sup>	882	860-900
Kinematic viscosity (40°C)	mm <sup>2</sup> /s	4.825	3.50-5.00
Acid number	mg KOH/g	0.16	<0.5
Iodine value	mg I <sub>2</sub> /100g	41.99	120
Water content	%	0.01	<0.05

### CONCLUSION

In summary, HA-Li600 catalyst had the highest surface basicity, amount of base sites, Lewis acid sites, and amount of Lewis acid sites, with the BET surface area of 10.5147 m<sup>2</sup>/g, and vibration of specific functional group O-Li shown at 1612.49 cm<sup>-1</sup>. The surface area of Li modified catalyst decreased with increased the average of particles size (179 to 392 nm) compared to the nanoparticle HA catalyst (97 nm). The SEM analysis indicated that morphology of the HA and HA-Li catalysts formed stack of agglomerates. The HA-Li600 catalyst had

more open and uniform pores than the others, hence the particles become unity one in others. The highest yield of biodiesel 88.16% was obtained using catalyst HA-Li600 with the ratio of 5%. The analysis of GC-MS showed 10 peaks, and 5 of the peaks with the highest percentage of area were identified as FAME derivative as followed: methyl oleic (25.37%), methyl palmitic (22.00%), methyl erusic (13.15%), methyl stearic (11.16%), and methyl linoleic (7.53%). The several physical and chemical properties of biodiesel were agreement with those reported by EN 14214 Standard.

**ACKNOWLEDGEMENT**

Thanks to the Directorate of Research and Community Service, Directorate General for Research and Development, the Ministry of

Research, Technology and Higher Education Republic of Indonesia through the Institute of Research and Community Service of Udayana University, for the Research Grant of Applied Product scheme year 2017.

**REFERENCES**

1. Xie, W. and Li, H., *Journal of Molecular Catalysis A: Chemical.*, **2006**, *255*, 1–9.
2. Lee, A.F.; Bennett, J.A.; Manayil, J.C.; and Wilson, K., *Chemical Society Reviews.*, **2014**, *43*, 7887-7916.
3. Atadashi, I.M.; Aroua, M.K.; Aziz, A.R.; and Sulaiman, N.M.N., *Journal of Industrial and Engineering Chemistry.*, **2013**, *19*(1), 14–26.
4. Guo, F. and Fang, Z., *Biodiesel Feedstocks and Processing Technologies.*, **2011**, 1–21.
5. Wang, K.; Guo, X.; Zhao, P.; Wang, F.; and Zheng, C., *J. Hazard Mater.*, **2011**, *189*, 301–307.
6. Refaat, A.A., *Int. J. Environ. Sci. Tech.*, **2011**, *8*(1), 203-221.
7. Simpen, IN. and Suastuti, N.G.A.M.D.A., *Indonesian Veterinary Journal.*, **2016**, *17*(4), 597-605.
8. Barakat, N.A.M.; Khil, M.S.; Omran, A.M.; Sheikh, F.H.; and Kim, H.Y., *Journal of Materials Processing Technology.*, **2009**, *209*, 3408–3415.
9. Wahl, D.A. and Czernuszka, J.T., *European Cell and Materials.*, **2006**, *11*, 43-56.
10. Park, J.H.; Lee, D-W.; I.M., S-W.; Lee, Y.H.; Suh, D-J; Jun K-W.; and Lee, K-Y., *Fuel.*, **2012**, *94*, 433-439.
11. Maaten, B.; Moussa, J.; Desmaretts, C.; Gredin, P.; Beaunier, P.; Kanger, T.; Tonsuaadu, K.; Villemin, D.; and Grussele, M., *Journal of Molecular Catalysis A: Chemical.*, **2014**, *393*, 112-116.
12. Hattori, H., *Appl. Catal.*, A-Gen., **2001**, *222*(1-2), 247-259.
13. Hattori, H., *Journal of the Japan Petroleum Institute.*, **2004**, *47*(2), 67-81.
14. Arpiwi, N.L.; Negara, IM.S.; and Simpen, IN., *J. Trop. Life Science.*, **2017**, *7*(3), 258-262.
15. Chen, K.T.; Wang, J.X.; Dai, Y.M.; Wang, P.H.; Liou, C.Y.; Nien, C.W.; and Chen, C.C., *Journal of the Taiwan Institute of Chemical Engineers.*, **2013**, *44*(4), 622–629.
16. Bobade, S.N. and Khyade, V.B., *Research Journal of Chemical Sciences.*, **2012**, *2*(7), 16-20.
17. Nasreen, S., Liu, H.; Skala, D.; Waseem, A.; and Wan, L., *Fuel Processing Technology.*, **2015**, *13*, 290-296.
18. Hindryawati, N.; Maniam, G.P.; Karim, M.R.; and Chong, K.F., *Engineering Science and Technology, an International Journal.*, **2014**, *17*(2), 95–103.
19. Betancur, A.I.G.; Arbelaez, D.G.E.; Lopez, A.d-R.; Malo, E.M.M.; Monoz, E.M.R.; Cortez, E.G.; Gomez, P.P.; Sandoval, S.J.; and Garcia, M.E.R., *Current Applied Physics.*, **2013**, *30*, 1-8.
20. Kongsri, S.; Janpradit, K.; Buapa, K.; Techawongstien, S.; and Chanthai, S., *Chemical Engineering Journal.*, **2013**, *215-216*, 522-532.
21. Essamlali, Y.; Amadine, O.; Larzek, M.; Len, C.; and Zahouily, M., *Energy Conversion and Management.*, **2017**, *149*, 355-367.